Causes of low thermospheric density during the 2007–2009 solar minimum

Stanley C. Solomon,[1] Liying Qian,[1] Leonid V. Didkovsky,[2] Rodney A. Viereck,[3] and Thomas N. Woods[4]

Received 27 January 2011; revised 22 March 2011; accepted 18 April 2011; published 13 July 2011.

[1] Satellite drag data indicate that the thermosphere was lower in density, and therefore cooler, during the protracted solar minimum period of 2007–2009 than at any other time in the past 47 years. Measurements indicate that solar EUV irradiance was also lower than during the previous solar minimum. However, secular change due to increasing levels of CO_2 and other greenhouse gases, which cool the upper atmosphere, also plays a role in thermospheric climate, and changes in geomagnetic activity could also contribute to the lower density. Recent work used solar EUV measurements from the Solar EUV Monitor (SEM) on the Solar and Heliospheric Observatory, and the NCAR Thermosphere-Ionosphere-Electrodynamics General Circulation Model, finding good agreement between the density changes from 1996 to 2008 and the changes in solar EUV. Since there is some uncertainty in the long-term calibration of SEM measurements, here we perform model calculations using the MgII core-to-wing ratio as a solar EUV proxy index. We also quantify the contributions of increased CO_2 and decreased geomagnetic activity to the changes. In these simulations, CO_2 and geomagnetic activity play small but significant roles, and the primary cause of the low temperatures and densities remains the unusually low levels of solar EUV irradiance.

Citation: Solomon, S. C., L. Qian, L. V. Didkovsky, R. A. Viereck, and T. N. Woods (2011), Causes of low thermospheric density during the 2007–2009 solar minimum, *J. Geophys. Res.*, *116*, A00H07, doi:10.1029/2011JA016508.

1. Introduction

[2] The solar cycle drives large temperature variation in the terrestrial thermosphere, primarily owing to the variation of solar irradiance in the extreme ultraviolet (EUV) and soft X-ray spectral range from 1 to 105 nm, here collectively referred to as solar EUV. This temperature change causes an even larger density variation in the upper thermosphere, with amplitudes of an order of magnitude near 400 km altitude, where many satellites orbit. Quantifying these density variations with empirical and theoretical methods is important for prediction of satellite trajectories, as they are influenced by atmospheric drag, particularly during high solar activity or geomagnetic storms. Conversely, analysis of the time evolution of satellite orbital elements provides a means by which the variation of thermospheric density can be measured, and has provided much of the data upon which empirical climatological models of thermospheric density are based.

[3] Superimposed on this solar-driven variation is a gradual decrease in temperature and density caused by increasing CO_2. *Roble and Dickinson* [1989] first predicted that a consequence of increasing CO_2 levels would be to decrease the temperature of the upper atmosphere, opposite to the response of the lower atmosphere. The reason for this apparent paradox is that CO_2 can emit infrared radiation as well as absorb it. Above the tropopause, the atmosphere becomes increasingly transparent to infrared radiation as densities decrease. CO_2 molecules are vibrationally excited by collisions, and spontaneously emit in the infrared, causing radiational cooling of the upper atmosphere. During the past decade, three different groups were able to measure long-term thermospheric density changes by observing the effect of atmospheric drag on satellites [*Keating et al.*, 2000; *Emmert et al.*, 2004; *Marcos et al.*, 2005]. The rate of change of density at a reference altitude of 400 km has been estimated to be between 2% and 5% per decade, in approximate agreement or slightly greater than model predictions [e.g., *Roble and Dickinson*, 1989; *Rishbeth and Roble*, 1992; *Akmaev and Fomichev*, 2000; *Qian et al.*, 2006]. In order to circumvent the problem of the complicating effects of the solar cycle, the initial findings by Keating et al. compared densities at successive solar minima. Theory [*Qian et al.*, 2006] and observation [*Emmert et al.*, 2004, 2008]

[1]High Altitude Observatory, National Center for Atmospheric Research, Boulder, Colorado, USA.
[2]Space Sciences Center, University of Southern California, Los Angeles, California, USA.
[3]Space Weather Prediction Center, NOAA, Boulder, Colorado, USA.
[4]Laboratory for Atmospheric and Space Physics, University of Colorado at Boulder, Boulder, Colorado, USA.

0148-0227/11/2011JA016508

agree that temperature and density change should be largest during solar minimum conditions, so if solar minima can be considered to have similar levels of solar EUV irradiance, and low geomagnetic activity, comparison of successive solar minima should provide a credible methodology for assessing anthropogenic global change in the thermosphere. Changes in the ionosphere accompany the neutral atmosphere changes, including slight changes in the height and peak density of ionospheric layers, and decreasing ion temperature. Recent reviews describe these and other possible effects, and assess the observational evidence [e.g., *Laštovička et al.*, 2006, 2008; *Qian et al.*, 2011].

[4] The descending phase of solar cycle 23 was long and gradual. By 2007, it appeared that solar minimum conditions had been reached, but recurrent geomagnetic activity and small oscillations in solar EUV irradiance continued [e.g., *Lei et al.*, 2008]. During 2008 and most of 2009, solar activity became extremely low, and the onset of solar cycle 24 was late and weak. A variety of parameters in the solar configuration and the near-Earth space environment indicated that conditions might be significantly quieter than the "usual" solar minimum [e.g., *Gibson et al.*, 2009; *Russell et al.*, 2010], and the long duration of the interval gave rise to additional speculation concerning long-term low–solar activity levels such as existed during the 1640–1700 period with few or no sunspots known as the "Maunder Minimum" [*Eddy*, 1976]. In late 2009, solar activity finally started to increase, but the 2 year period between mid-2007 and mid-2009 was one of the longest of recent solar minima. There is now good evidence from space-based measurements that the solar EUV irradiance was also anomalously low during this time, or at least lower than the previous solar minimum [*Didkovsky et al.*, 2010].

[5] Identification of anomalous conditions in near-Earth space during the summer of 2008 was provided by *Heelis et al.* [2009], who analyzed space-based ionospheric measurements from the Coupled Ion Neutral Dynamics Investigation (CINDI), showing that ion temperatures and the O^+/H^+ transition height were both lower than expected. *Coley et al.* [2010] further described the equatorial distribution of these parameters, and validated the observations with radar data from the Jicamarca observatory. *Lühr and Xiong* [2010] confirmed these ionospheric results using data from the CHAMP and GRACE satellites, and *Chen et al.* [2011] found a significant decrease in ionosonde measurements of peak ionospheric densities during the cycle 23/24 minimum, compared to previous solar minimum periods. However, the clearest and most compelling evidence concerning the anomalous nature of this solar minimum comes from the neutral atmosphere. Long-term measurements of the global mean neutral density measurements by *Emmert et al.* [2010] found that thermospheric density during this solar minimum period was significantly lower (at constant altitude levels) than the previous three, and well below the expected secular trend. *Bruinsma and Forbes* [2010] showed that CHAMP accelerometer measurements also support the lower, cooler state of the thermosphere-ionosphere system.

[6] Recent work [*Solomon et al.*, 2010] attempted to explain the thermospheric density changes between 1996 and 2008 using EUV measurements [*Didkovsky et al.*, 2010] to estimate synthetic solar spectral input to the NCAR Thermosphere-Ionosphere-Electrodynamics General Circulation Model (TIE-GCM). The integrated energy flux in the spectrum derived for 2008 was 13% lower than for 1996, which resulted in good agreement with the magnitude of density reduction. However, in that preliminary study, comparisons were performed using a single solar EUV spectrum as characteristic of each minimum period, the model was only run for a few months, and geomagnetic activity effects were neglected. The more comprehensive approach taken in the present work is to perform full-year runs, including geomagnetic effects as well as changes due to CO_2 cooling, and specifying daily solar EUV variation using the MgII core-to-wing ratio index [*Viereck et al.*, 2004, 2010]. The purpose of this study is to confirm that low solar EUV irradiance is the primary cause of the anomalously low thermospheric density, but also to quantify the roles played by other contributing factors.

2. Data Analysis

2.1. Data Sources

[7] Global average thermospheric total mass density is derived from the effect of atmospheric drag on objects orbiting Earth [*Emmert et al.*, 2008; *Emmert*, 2009] through analysis of their orbital elements. Up to 5000 orbiting objects are employed. Density is obtained at several reference altitudes; here, results are referenced to 400 km. Although the solar EUV irradiance is the most important parameter affecting thermospheric density, short-term perturbations from geomagnetic activity, periodic seasonal variations due to changes in atmospheric circulation and mixing, and the Sun-Earth distance, are also significant [*Qian et al.*, 2009]. These may be removed using empirical reference models [*Emmert et al.*, 2010] in order to focus on the solar effect, but in the analysis shown here, unadjusted mass densities are employed. Figure 1a is a plot of daily mean thermospheric density since 1970, at 400 km altitude. The 81 day centered running mean and the annual mean for each year are also plotted, showing that 2007, 2008, and 2009 were the three lowest-density years on record, and 2008 was ~30% lower than the solar cycle 22/23 minimum in 1996. The overall uncertainty in these data is estimated to be 10%, and the long-term stability of the measurement is estimated to be 3% [*Emmert et al.*, 2008]. The slight decline in each successive minimum, attributed to increasing CO_2 levels, is apparent, but the solar cycle 23/24 annual minimum values were well below that trend.

[8] Solar EUV measurements and solar proxy indices could be useful for understanding these changes, but only a few are available that span the 14 year period from 1996 through 2009. Measurements of solar EUV levels are available from several space-based experiments, including the Solar EUV Monitor (SEM) [*Judge et al.*, 1998] on the Solar and Heliospheric Observatory (SOHO), the Solar EUV Experiment (SEE) [*Woods et al.*, 2005] on the Thermosphere-Ionosphere-Mesosphere Energetics and Dynamics (TIMED) satellite, and several suborbital rocket flights used to calibrate these instruments. Additional broadband measurements in the soft X-ray region are available from the Student Nitric Oxide Explorer (SNOE) and Solar Radiation and Climate Experiment (SORCE) [*Bailey et al.*, 2000; *Solomon et al.*, 2001; *Woods and Rottman*, 2005]. However,

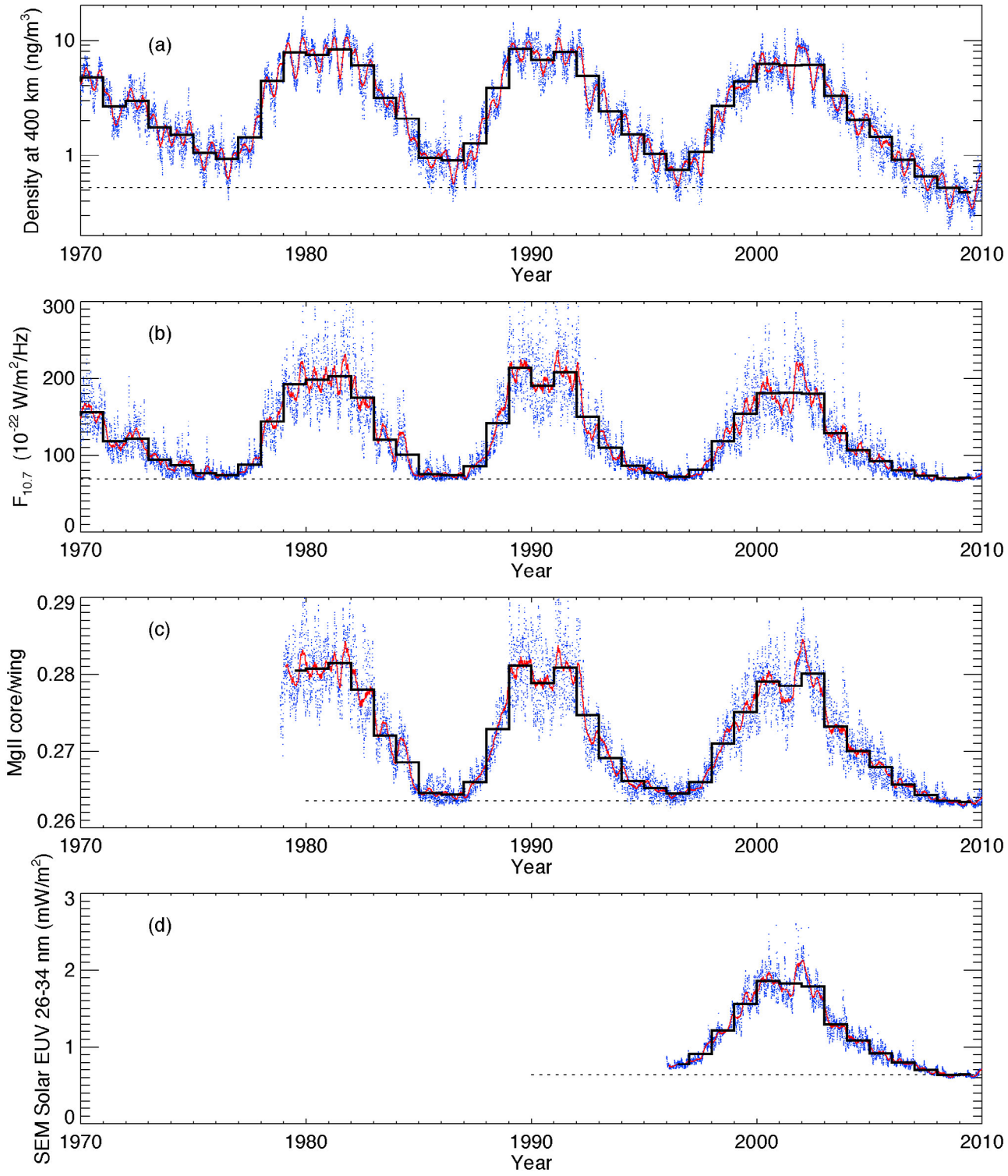

Figure 1. Time series of thermospheric density measurements, solar indices, and solar EUV measurements. (a) Global mean thermospheric density at 400 km altitude, obtained from satellite orbital parameters over four solar cycles [after *Emmert et al.*, 2010]. (b) $F_{10.7}$ solar proxy index. (c) MgII core-to-wing ratio solar proxy index. (d) Solar EUV energy flux in the 26–34 nm band measured by the SEM detector on the SOHO spacecraft [after *Didkovsky et al.*, 2010]. Blue dots, daily mean values; red lines, 81 day centered running means; solid black lines, annual means; black dashed lines, 2008 annual means.

only the SEM has made measurements spanning the two most recent solar minima. The primary SEM data product is the integrated solar EUV flux in the 26–34 nm band, which contains the bright He II line at 30.4 nm and several important coronal lines, comprising about a quarter of the total solar EUV energy flux.

[9] The 10.7 cm solar radio flux index $F_{10.7}$ is a widely used proxy that correlates well with general solar activity and with EUV and UV emissions. It has considerable heritage in solar and upper atmosphere empirical models, and is available nearly continuously since 1947. However, there are issues with its behavior during solar minimum conditions, as discussed in section 2.2. The core-to-wing ratio of the magnesium ion *h* and *k* lines at 279.56 and 280.27 nm (MgII core-to-wing ratio (c/w)) has been shown to be a good measure of solar chromospheric activity, and is a valuable proxy for solar flux at many EUV wavelengths [*Viereck et al.*, 2004]. It is calculated by taking the ratio between the highly variable chromospheric lines and the weakly varying photospheric wings. Measurement sources include several space-based data sets, including the NOAA Solar Backscatter Ultraviolet (SBUV) instruments, the Upper Atmosphere Research Satellite (UARS) solar observations, the Global Ozone Monitoring Experiment (GOME), the Scanning Imaging Absorption Spectrometer (SCIAMACHY), and SORCE. The data are intercalibrated and combined into a daily index by *Viereck et al.* [2004, 2010].

[10] Figure 1b is a plot of the $F_{10.7}$ solar radio flux at 1 AU, obtained from the National Geophysical Data Center (NGDC). At solar minimum, $F_{10.7}$ generally reaches a plateau while solar EUV irradiance continues to exhibit small variations [e.g., *Barth et al.*, 1990; *Woods et al.*, 2000]; in 2008–2009, this plateau was slightly below the preceding minima, with an annual average for 2008 of 69, as compared to an annual average for 1996 of 72. This change is ~2% of the historical range of smoothed $F_{10.7}$ values (typically 70 to 220), which is too small a change to explain the lower thermospheric densities. *Emmert et al.* [2010] estimate that a change in thermospheric density of only ~10% could be expected from this deviation in the $F_{10.7}$ index on the basis of empirical models. In Figure 1c, the MgII c/w index is plotted from its inception in 1978 through 2009. Unlike the $F_{10.7}$ index, MgII c/w does show a significant decline from 1996 to 2008, from an annual average value of 0.2645 to 0.2635, or ~5% of its historical range of smoothed values (typically 0.264 to 0.283). Also unlike the $F_{10.7}$ index, MgII c/w does not stop varying below a constant plateau at solar minimum, but usually continues to exhibit some variation, as can be seen during 1985–1986 and 1995–1996. During 2007–2009, much of that variation ceased, but the fairly constant values during 2008 were similar to the envelope of the minimum values from previous minima. This provides some evidence that MgII c/w could be a superior proxy for solar EUV, especially during solar minimum. The SEM results from 1996 to 2010 at 1 AU [*Didkovsky et al.*, 2010] are shown in Figure 1d. Didkovsky et al. describe their calibration using similar instruments on eight rocket flights, document a 6% estimated uncertainty, and estimate a reduction of 15% in solar flux measured within this wavelength band from the minimum between solar cycles 22/23 to the minimum between solar cycles 23/24. There is some independent confirmation of these changes from other suborbital flights, and from TIMED/SEE [*Woods et al.*, 1998, 2005, 2009; *Chamberlin et al.*, 2009], but the uncertainty estimates for these measurements are significant, as discussed by *Solomon et al.* [2010].

2.2. Intercomparison of Data

[11] Given the various behaviors of these measurements and proxy indices (which, of course, are based on measurements as well) at solar minimum, it is necessary to perform some comparisons in order to investigate their consistency. Annual averages are employed for these comparisons, because they reduce random variation, integrate over a range of geomagnetic activity levels, and remove systematic seasonal effects. Seasonal changes, from a variety of causes, are particularly prominent in the neutral density data [cf., *Qian et al.*, 2009] and can be discerned by inspection of Figure 1a. In Figure 2, annual mean values of global mean densities at 400 km altitude (Figures 2a and 2b), and the SEM 26–34 nm solar EUV flux (Figures 2c and 2d), are plotted against $F_{10.7}$ (Figures 2a and 2c) and MgII c/w (Figures 2b and 2d). The ascending phase of solar cycle 23 from 1996 to 2001 is shown in red, and the descending phase from 2002 to 2009 is shown in blue.

[12] Several observations may be made from these comparisons. The first, and most important, is that all measurements agree that the 2008 (and 2009) annual averages were lower than 1996. However, as noted in section 2.1, the $F_{10.7}$ index was only slightly lower during these 2 years, while the other measurements showed larger deviation. The comparison of density to $F_{10.7}$ is quite consistent between ascending and descending phases through 2005, following a reasonably smooth curve, and only starts to diverge slightly during 2006 and 2007. However, $F_{10.7}$ variation past 2007 is small, while the density change is considerable. By contrast, the MgII c/w continues to decline after 2007, and appears to vary with thermospheric density in a consistent manner. Near solar maximum, the ascending versus descending correspondence is not as good, but for 1996–1999 and 2003–2007 the comparison is quite satisfactory, with the descending averages lying just below the ascending curve, as might be expected from cooling due to CO_2 change. SEM measurements were compared to thermospheric densities by *Solomon et al.* [2010, Figure 3b] showing approximate consistency, but slightly lower solar EUV for a given density level, during the later years of the declining phase. Here, we compare SEM data to $F_{10.7}$ and MgII c/w, showing that SEM is lower compared to both indices during 2005–2009 than the comparative curve established during 1996–1998. As with the comparison to density data, the $F_{10.7}$ index "plateaus" during solar minimum while the solar EUV continues to decline. The comparison with MgII c/w does not suffer from this issue, showing a reasonably linear trend throughout the declining phase despite the slight offset from the ascending phase.

2.3. Using the MgII c/w Index for Solar EUV Calculations

[13] This analysis does not reveal the existence of an ideal solar observation or proxy index, but it does point out the

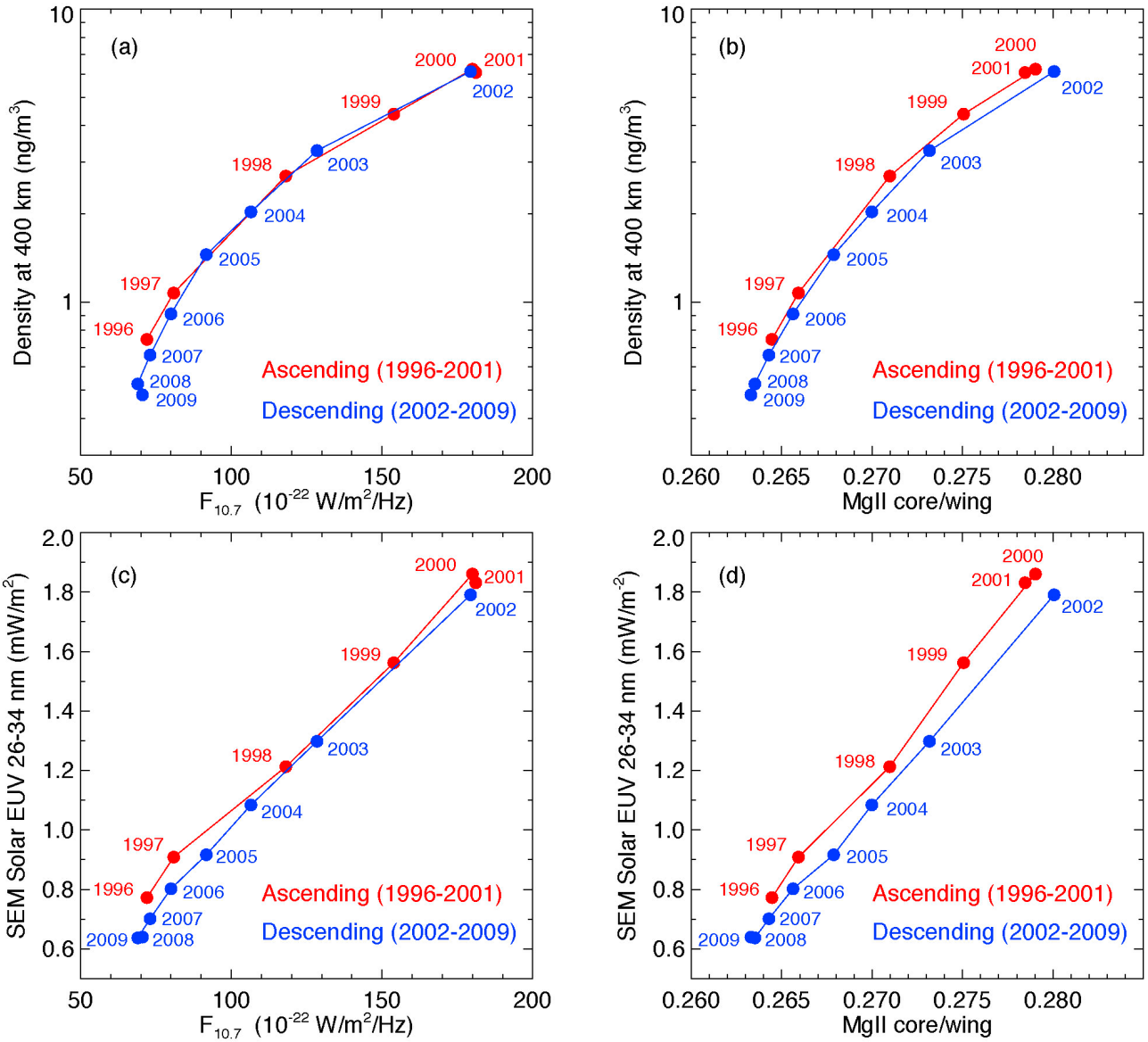

Figure 2. Comparison of thermospheric global mean density annual averages and solar EUV annual averages to solar proxy indices during solar cycle 23. Red lines, ascending phase (1996–2001); blue lines, descending phase (2002–2009).

uncertainties in some of them. $F_{10.7}$ is valuable for its consistency and longevity, but it has long been known to have problems at solar minimum [e.g., *Barth et al.*, 1990], and these problems appear to be exacerbated by the particular conditions of the minimum between solar cycle 23/24. SEM is the longest-running actual solar EUV measurement, and has been repeatedly recalibrated using suborbital observations [*Didkovsky et al.*, 2010], but long-term calibration of solar EUV measurements is notoriously difficult, and the stability accuracy estimate of 6% allows for a significant range of solar minimum values. Therefore, it is worth investigating how well MgII c/w performs for this anomalous solar minimum. In order to do so, an ad hoc method was developed for employing MgII c/w in standard solar EUV proxy models. Daily average values of $F_{10.7}$ were compared to MgII c/w during 1978–2007, and an unweighted linear least squares fit of $F_{10.7}$ to MgII c/w performed, resulting in the relationship:

$$M_{10.7} = 7984(\text{MgII c/w}) - 2041 \quad (1)$$

where $M_{10.7}$ is the MgII c/w scaled to $F_{10.7}$, in units of 10^{-22} W m^{-2} Hz^{-1}. Figure 3a shows these data and the linear fit. Data from 2008 to 2009 were excluded from the fit, in order to avoid biasing the result using the anomalous solar minimum period we are attempting to describe. Nevertheless, the effect of previous solar minima may be clearly seen on this plot at the lower values; this is due to the plateau behavior of $F_{10.7}$ discussed in section 2.2. A linear fit appears to be a reasonable approximation away from

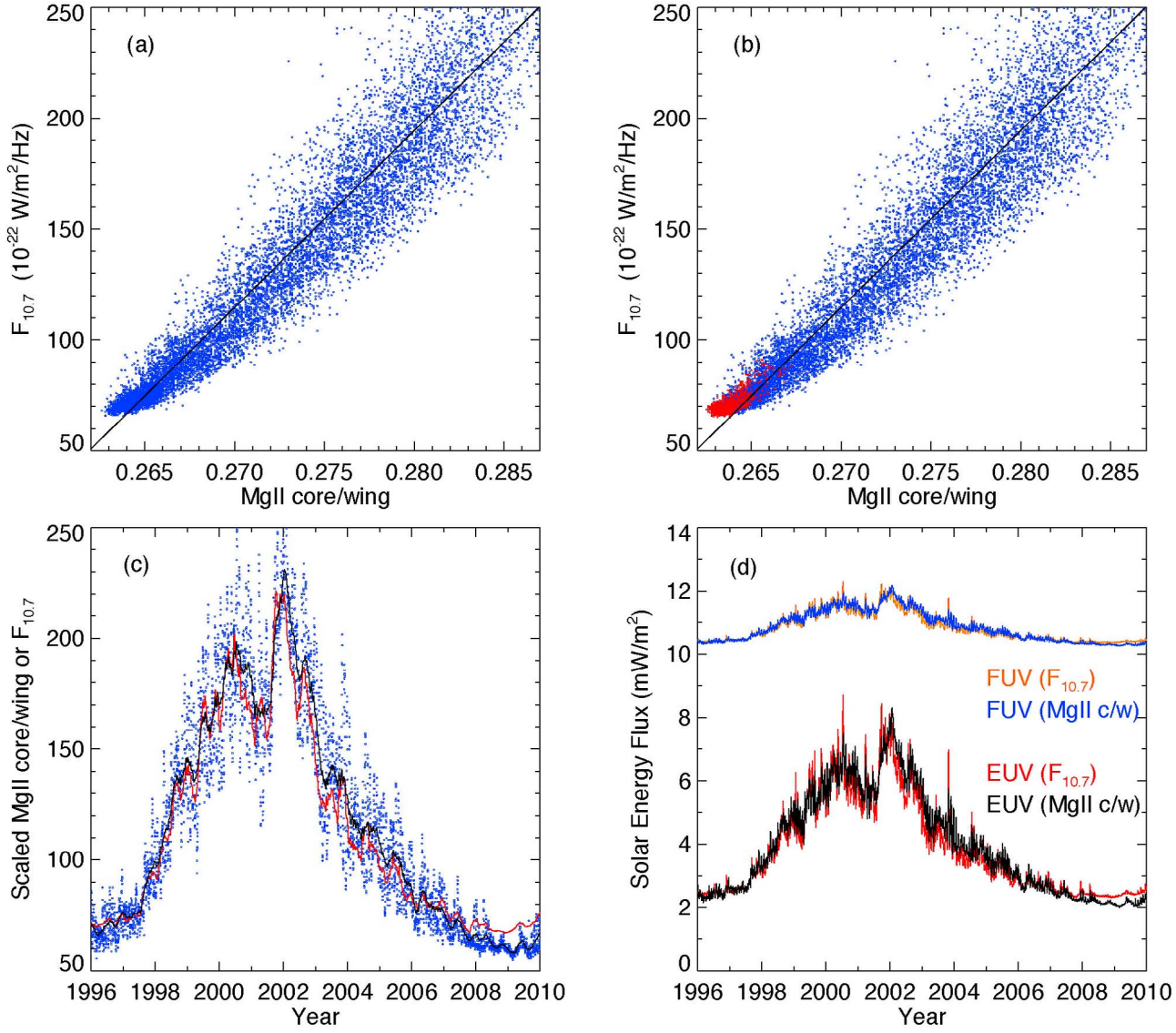

Figure 3. Comparison of the $F_{10.7}$ and MgII core-to-wing ratio (c/w) solar proxy indices and the resulting solar energy fluxes calculated using these indices in empirical models. (a) $F_{10.7}$ versus MgII c/w during 1978–2007. Blue dots, daily mean values; black line, linear fit of $F_{10.7}$ to MgII c/w, $M_{10.7}$ = 7984(MgII c/w) − 2041. (b) Same as Figure 3a but with 2008–2009 values also plotted in red. (c) Scaled MgII c/w ($M_{10.7}$), for solar cycle 23. Blue dots, daily mean $M_{10.7}$; black line, 81 day centered running mean of $M_{10.7}$; red line, 81 day centered running mean of $F_{10.7}$. (d) Solar energy flux calculated by empirical models using scaled MgII c/w and using $F_{10.7}$ for solar cycle 23. Black line, EUV energy flux (0–105 nm) using scaled MgII c/w as input to the EUVAC model; red line, EUV energy flux (0–105 nm) using $F_{10.7}$ as input to the EUVAC model; blue line, FUV energy flux (125–175 nm) using MgII c/w as input to the *Woods and Rottman* [2002] model; orange line, FUV energy flux (125–170 nm) using $F_{10.7}$ as input to the *Woods and Rottman* [2002] model.

these low values, and so was chosen instead of a higher-order polynomial, because this low-end curvature is precisely the behavior of $F_{10.7}$ that we are trying to eliminate by using an index that may have a more linear relationship with actual solar EUV levels. The 2008–2009 values are included, in red, in Figure 1b. It is apparent that these points conform to a pattern seen in previous solar minima, but there are more of them, owing to the extended duration of solar minimum conditions. In Figure 1c, the values of MgII c/w scaled to $F_{10.7}$ using the linear fit; that is, $M_{10.7}$, are shown for solar cycle 23. The blue dots are the daily mean $M_{10.7}$, and the black line is its 81 day centered running mean. The 81 day centered running mean of $F_{10.7}$ is also shown, in red, for comparison.

[14] The standard solar EUV irradiance input to the NCAR TIE-GCM (described in section 3) is provided by the EUVAC proxy model [*Richards et al.*, 1994]. The model is

Table 1. Annual Mean Values of Solar EUV Derived Using EUVAC

Year	EUV From $F_{10.7}$ (W m^{-2})	EUV From $M_{10.7}$ (W m^{-2})	Ratio M_{EUV}/F_{EUV}
1996	2.49	2.44	0.98
2008	2.39	2.20	0.92
Ratio 2008/1996	0.96	0.90	

extended below 5 nm as described by *Solomon and Qian* [2005]. Individual bands and lines of solar EUV photon flux are calculated by EUVAC as linear functions of the input variable P, which is defined as the average of the daily $F_{10.7}$ and its running 81 day centered mean. Therefore, for purposes of these calculations, we simply calculated P using $M_{10.7}$ and its 81 day mean, and used it as input to EUVAC. Similarly, far ultraviolet (FUV) irradiances are provided by the *Woods and Rottman* [2002] model, which also employs daily $F_{10.7}$ and its 81 day mean; these values were also calculated by substituting $M_{10.7}$. The results of these calculations are shown in Figure 3d. The EUV integrated energy flux calculated using $M_{10.7}$ (in black) is compared to values calculated in the standard way using $F_{10.7}$ (in red). The annual mean EUV energy flux derived from $M_{10.7}$ is 10% lower in 2008 than in 1996, as compared to only 4% lower using $F_{10.7}$, as shown in Table 1. The FUV flux (here excluding the H Lyman α emission line at 121.6 nm) has much less variability, and hence is only slightly different for the two input proxies, but is also shown in Figure 3d, and included in the model runs below, for completeness.

3. Model Simulations

[15] Model simulations were performed to investigate the relative contributions to thermospheric density reduction of solar EUV, geomagnetic activity, and increasing CO_2 levels. The NCAR Thermosphere-Ionosphere-Electrodynamics General Circulation Model (TIE-GCM) v. 1.93 [*Roble et al.*, 1988; *Richmond et al.*, 1992] is the primary model employed here. The TIE-GCM is a first-principles upper atmospheric general circulation model that solves the Eulerian continuity, momentum, and energy equations for the coupled thermosphere-ionosphere system. It uses pressure surfaces as the vertical coordinate and extends in altitude from approximately 97 km to 600 km. The solar input was derived from the MgII c/w, the EUVAC model, and the Woods and Rottman model, as described in section 2.3, and applied to the TIE-GCM using the method of *Solomon and Qian* [2005]. Tidal forcing at the lower boundary was specified by the Global Scale Wave Model [*Hagan et al.*, 2001], and semiannual and annual density periodicities were obtained by applying seasonal variation of the eddy diffusivity coefficient at the lower boundary [*Qian et al.*, 2009]. The CO_2 mixing ratio imposed at the lower boundary was 360 ppmv for 1996 and 385 ppmv for 2008, based on measurements from the Mauna Loa Observatory [*Keeling and Whorf*, 2005]. The model was run for each full year for two different cases: one run with variable geomagnetic activity specified by the 3 h *Kp* index, and another run with *Kp* set to a value of 0.5, effectively eliminating the effects of high-latitude forcing from magnetospheric convection and auroral precipitation. The lower-boundary conditions were the same for all four runs.

[16] Figure 4 shows the results of these simulations for 1996 and 2008 on day of year 227, at 12 UT. The full simulation, including geomagnetic forcing, and CO_2 change, is presented. The left column displays temperature and the right column displays density, both at the reference altitude of 400 km. Figures 4a and 4b are the 1996 simulation, Figures 4c and 4d are the 2008 simulation, and Figures 4e and 4f show the temperature difference and density ratio as a function of geographic latitude and longitude, respectively.

[17] For comparison, simulations were also performed for each day of both years using the NRLMSISE-00 empirical model [*Picone et al.*, 2002]. Similar to the approach employed for running EUVAC, the scaled $M_{10.7}$ values and its 81 day average were substituted for $F_{10.7}$ in performing the model runs. This approach is taken as an approximation to the solar minimum behavior, and is not suggested for calculations throughout the solar cycle, owing to nonlinearity in the way that NRLMSISE-00 uses $F_{10.7}$ to estimate the exospheric temperature. The daily *Ap* index was used as input for the run with variable magnetic activity, and *Ap* was set to a value of 3 for the constant magnetic activity test.

3.1. Density Changes Caused by Solar EUV

[18] Figure 5 plots time series of daily average density at 400 km altitude from model simulations, compared to satellite drag measurements. Simulations with geomagnetic activity included (red) and excluded (blue) are plotted, along with the daily *Ap* index (divided by 100) for reference. Figure 5a shows the results for the TIE-GCM in 1996, Figure 5b shows TIE-GCM results for 2008, Figure 5c shows NRLMSISE-00 results for 1996, and Figure 5d shows NRLMSISE-00 results for 2008. The systematic offset between 1996 and 2008 is apparent in both comparisons. The TIE-GCM does a reasonable job of tracing the baseline of the observations with geomagnetic activity turned off, although NRLMSISE-00 is a little higher, owing to known issues with this model in replicating solar minimum densities. However, the relative change between 1996 and 2008 is similar in both models, a ~22% reduction due to solar EUV change alone.

3.2. Density Changes Caused by Geomagnetic Activity

[19] Both TIE-GCM and NRLMSISE-00 represent the variations in global mean density driven by geomagnetic activity quite well, although the amplitude in both simulations is slightly smaller than the data. Overall geomagnetic activity during 2008 was modestly reduced compared to 1996 (annual average $Ap = 7$ in 2008 as opposed to $Ap = 9$ in 1996). This can be discerned, barely, in Figure 5. Given the low levels of geomagnetic activity, and the small changes between the two solar minima, it is expected that the modeled density changes due to this factor will be small. They are calculated by comparing the annual mean differences with and without geomagnetic activity for the two years, resulting in 2.2% reduction derived from TIE-GCM simulations, and 3.5% derived from NRLMSISE-00. Use of the daily *Ap* to run NRLMSISE-00 adds a small lag from the model calculation to the measurement, evident in Figures 5c and 5d.

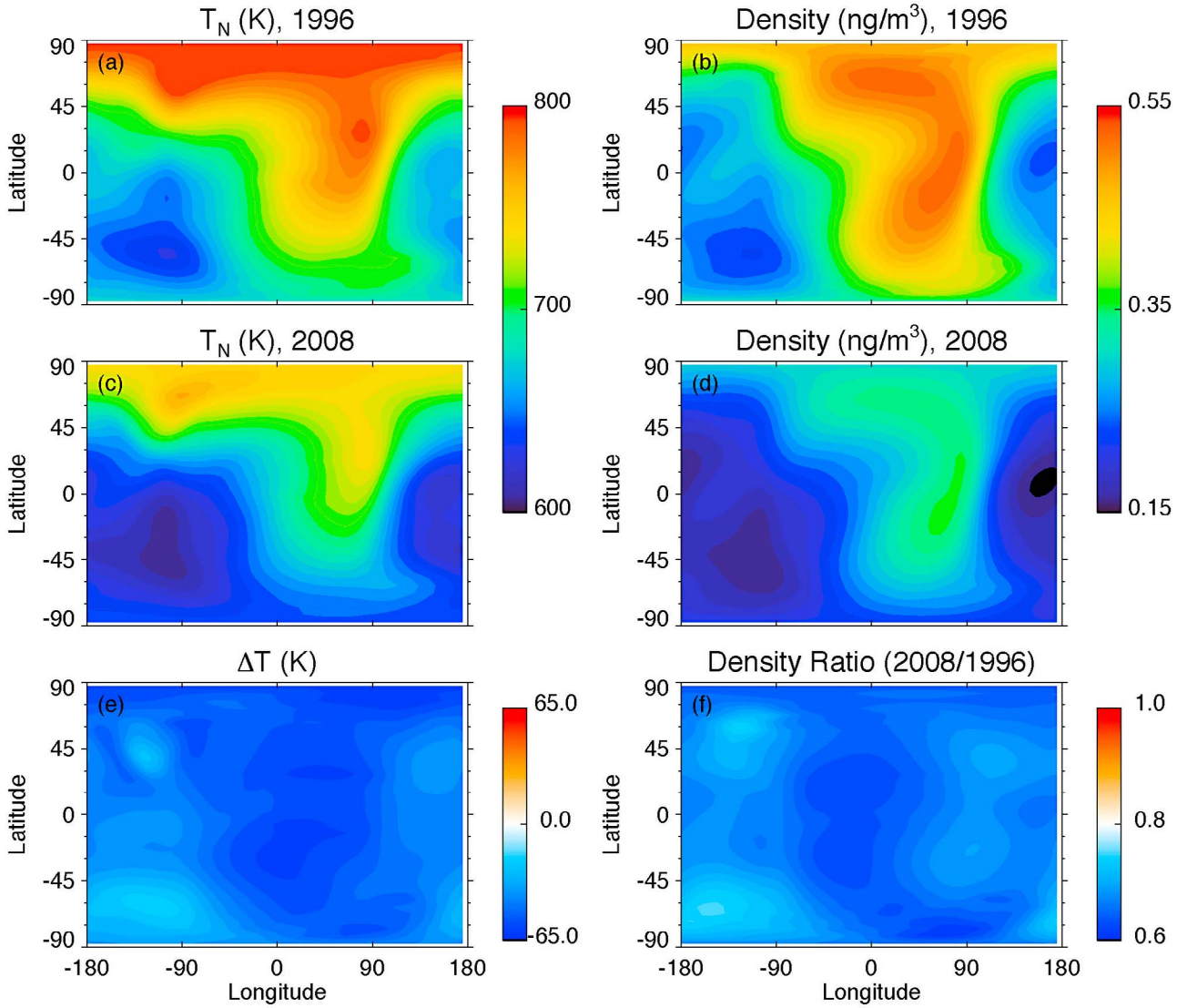

Figure 4. Thermospheric temperature and density modeled by the NCAR TIE-GCM for 1996 and 2008, on day of year 227, using the scaled MgII c/w proxy index $M_{10.7}$ as input (see Figures 3c and 3d). (a) Model temperature at 400 km for 1996. (b) Model density at 400 km for 1996. (c) Model temperature at 400 km for 2008. (d) Model density at 400 km for 2008. (e) Temperature difference at 400 km for 2008/1996. (f) Density ratio at 400 km for 2008/1996.

[20] Figure 6 shows the altitude dependence of the temperature and density changes calculated by the TIE-GCM, with and without the effects of geomagnetic activity. Global annual averages are plotted, showing the effect of including (red line) and neglecting (blue line) geomagnetic activity. This shows that the change due to increased geomagnetic activity, while significant and measurable, is much smaller than the change due to solar input. At 400 km, the combined decrease in temperature is 40 K, 7 K of which is attributable to decreased geomagnetic activity, and the combined decrease in density is 27%, 2.2% of which is attributable to decreased geomagnetic activity. The temperature change caused by geomagnetic activity is relatively large compared to density change; this is because of the compensating effect of composition variation, since the atomic oxygen to molecular nitrogen ratio in the upper thermosphere increases with decreasing geomagnetic activity. Also plotted in Figure 6d are the density changes as a function of altitude derived by *Emmert et al.* [2010]. The measured density changes are a few percentage points larger than the modeled changes, but the slope of the changes is very similar, indicating that the basic physical mechanisms employed by the model are at least commensurate with the observations.

3.3. Density Changes Caused by CO_2

[21] The component of these changes attributable to increasing CO_2 concentration was investigated by *Solomon et al.* [2010], so the calculations are not repeated here. Those

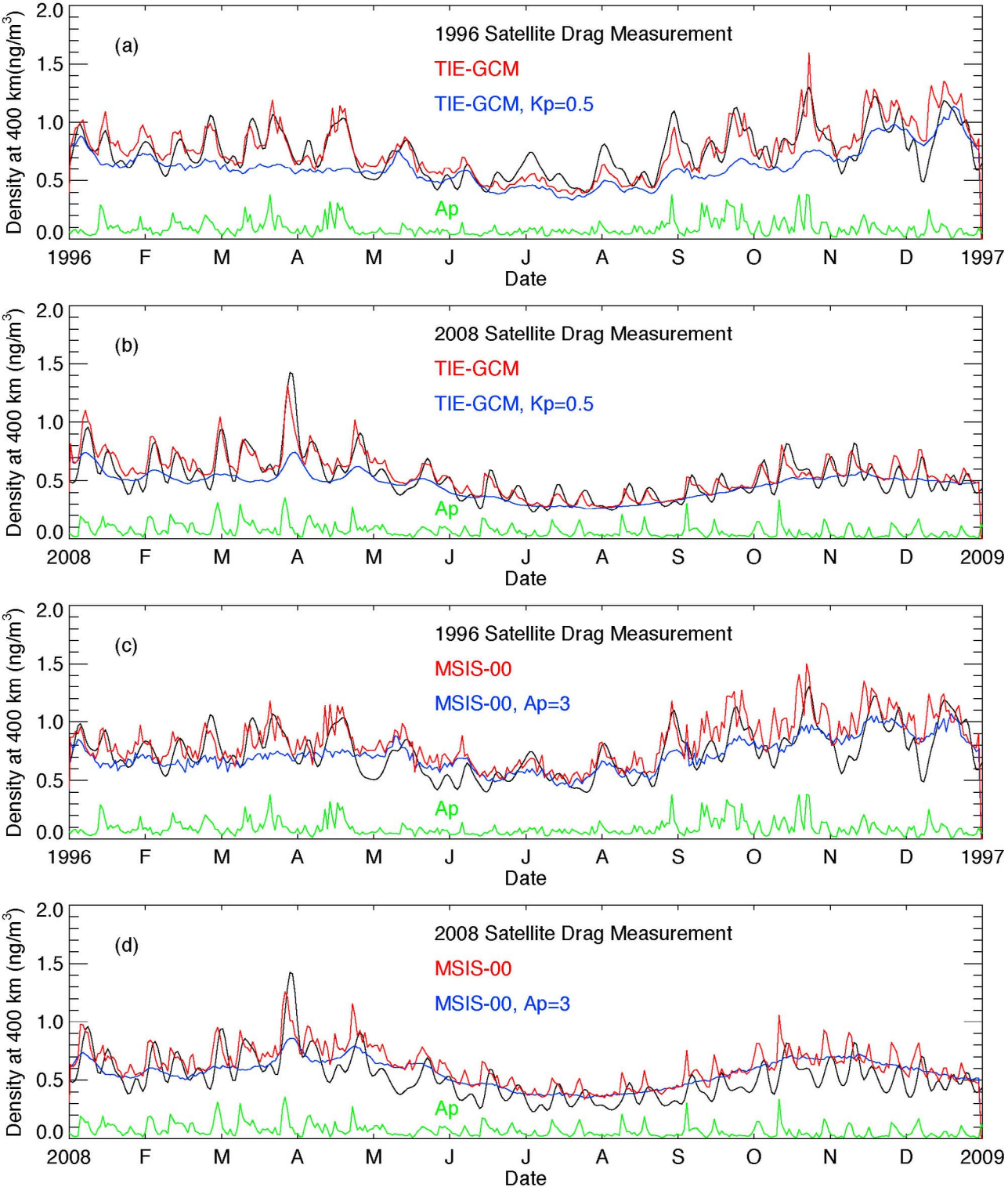

Figure 5. Time series of daily global mean model simulations, using scaled MgII c/w as input, compared to thermospheric density measurements at 400 km. (a) TIE-GCM and density for 1996. (b) TIE-GCM and density for 2008. (c) NRLMSISE-00 and density for 1996. (d) NRLMSISE-00 and density for 2008. Black lines, global mean thermospheric density measurements; red lines, daily mean model simulations; blue lines, model simulations, excluding the effects of geomagnetic activity by setting the driving input parameters to constant, very low values; green lines, daily *Ap* geomagnetic index, divided by 100, for comparison.

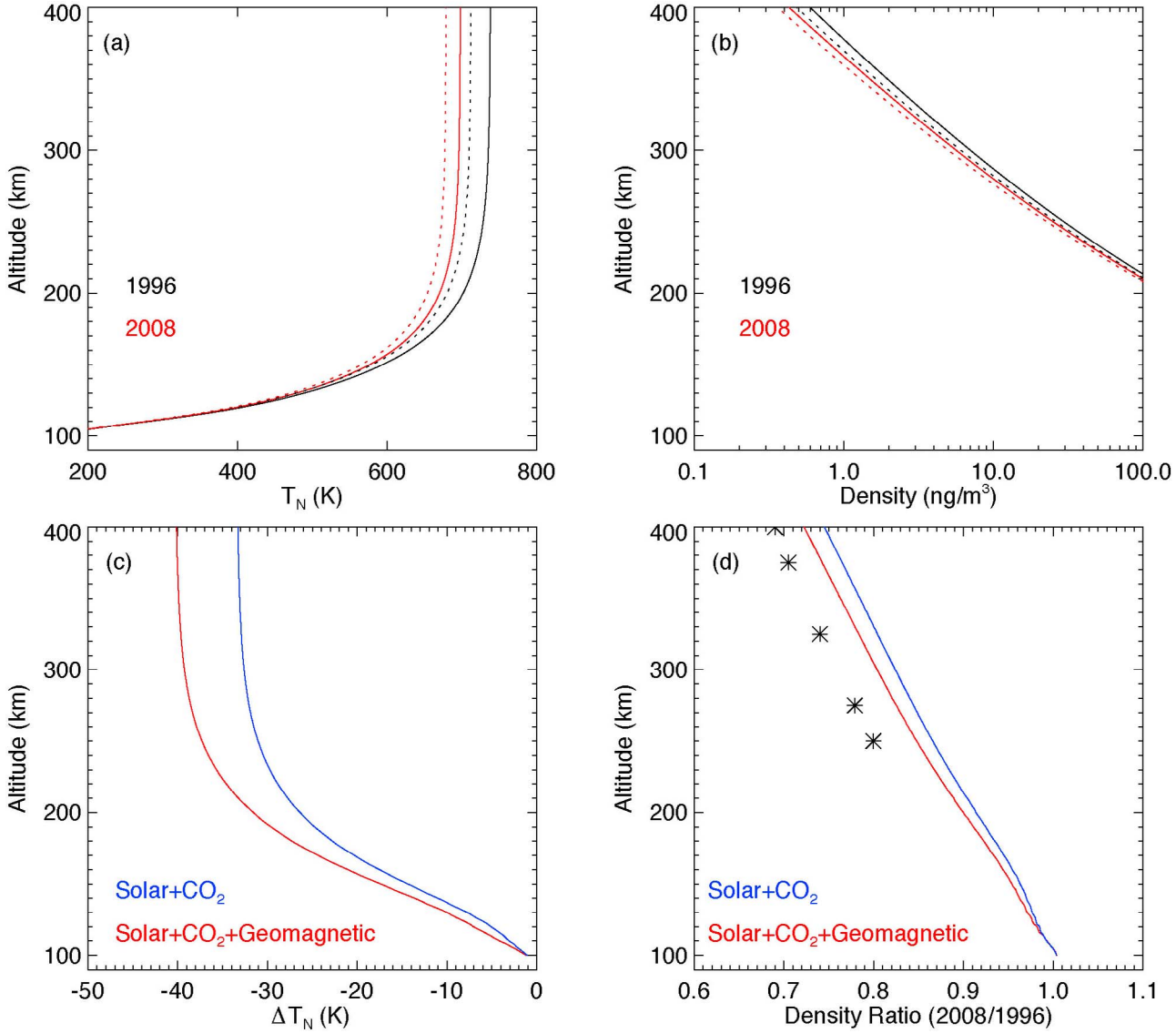

Figure 6. Altitude profiles of global annual mean temperatures and densities derived from the TIE-GCM simulations shown in Figures 4 and 5. (a) Temperature profiles. Solid red and black lines, model simulations including the effects of all known changes, including solar irradiance, CO_2 change, and geomagnetic activity; dashed red and black lines, the same model simulations but excluding the effects of geomagnetic activity. (b) Density profiles (lines are the same as in Figure 6a). (c) Temperature change profiles for 2008–1996. Red line, model simulations including the effects of all known changes; blue line, the same model simulations but excluding the effects of geomagnetic activity. (d) Density ratio profiles for 2008/1996 (lines are the same as in Figure 6c). Asterisks indicate density ratios derived from satellite drag data as a function of altitude by *Emmert et al.* [2010].

findings were commensurate with the calculations of *Qian et al.* [2006], that the effect of CO_2 mixing ratio in the lower atmosphere increasing from 360 to 385 ppmv over the 12 years from 1996 to 2008 should cause a decrease in thermospheric density at 400 km of ~3% under solar minimum conditions. However, we note that observational estimates of this change run as high as 5% per decade, or as much as 6% between the two solar minima. The effects due to CO_2 are included in both of the TIE-GCM simulations shown in Figures 5 and 6, but not in the NRLMSISE-00 calculations, since NRLMSISE-00 does not yet include a secular term.

4. Conclusions

[22] The results of these simulations are summarized in Table 2, where the individual components of change attributable to the three known sources are derived from the model simulations, and compared to satellite drag measurements. The TIE-GCM results are similar to preliminary

Table 2. Annual Mean Density Changes at 400 km Altitude From 1996 to 2008

	Solar EUV (%)	Geomagnetic (%)	CO_2 Cooling (%)	Total (%)
Satellite drag data				−30
NCAR TIE-GCM	−22	−2.2	−3	−27
NRLMSISE-00	−21	−3.5	NA[a]	−25

[a]NA, not applicable.

work by *Solomon et al.* [2010] using SEM data, constant solar input, shorter model runs, and neglecting geomagnetic variation. Since the solar EUV change assumed here averages 10%, as opposed to the 13% employed in the previous study, the simulated change due to solar EUV is proportionally smaller, 22% instead of 28%. This is partially compensated by the addition of geomagnetic variation, resulting in reasonable agreement with the observed changes. Since it is possible that the TIE-GCM slightly underestimates the geomagnetic component and the CO_2 cooling component, we note that increasing these by a few percentage points would bring the TIE-GCM simulations into even better agreement with observations. The NRLMSISE-00 simulations are included here despite the vagaries involved in using a substitute index in this model, to see if the TIE-GCM results are basically compatible with empirical models, and as a check on the geomagnetic activity estimation. The models do indeed give similar results, and although NRLMSISE-00 produces somewhat higher change in density due to geomagnetic forcing, in both cases this is still a small portion of the total. Reduction in density due to increased CO_2 cooling is not included in the NRLMSISE-00 results, but adding in −3% to −6% secular change would bring them quite close to the observations.

[23] The uncertainties in the TIE-GCM simulations are considerable, deriving from four primary sources. The first of these is simply the general uncertainty in what solar EUV levels really were, and how much they changed between the two solar minima. Then, by using the MgII c/w rescaled to $M_{10.7}$ additional error is introduced, since MgII c/w is a composite index derived from multiple data sets, and the relationship between MgII and $F_{10.7}$ cannot be perfectly linear, even in the absence of measurement and calibration errors. Model parameterizations of heating rates, chemical terms, heat conduction, and cooling rates, are always a work in progress, although considerable effort has gone into obtaining an accurate relationship between model simulations and neutral density measurements over solar cycle 23 [e.g., *Qian et al.*, 2009]. Finally, the parameterization of magnetospheric convection and auroral precipitation by the *Kp* index is only an approximate substitute for specific knowledge of these inputs, and the resulting calculation of high-latitude Joule heating is known to be fraught with peril. Given all of this, it is perhaps surprising that a good correspondence with density changes derived from satellite drag observations can be obtained at all. Excluding the uncertainties in model inputs, we estimate the intrinsic uncertainties in the TIE-GCM and in NRLMSISE-00 to be similar, on the order of 15%. However, the primary conclusion of this work is not a precise inference of solar change or density change, but rather that the physical mechanisms of solar energy deposition, magnetospheric energy transfer, and anthropogenic changes to the radiation balance, can be explicated, in order to understand their relative importance.

[24] It is noteworthy that geomagnetic activity became extremely low in mid-2008, and remained low until late 2009, spanning about 1.5 years of some of the quietest solar terrestrial conditions ever observed. Consequently, 2009, with an annual average $Ap = 4$, was slightly lower in annual average density than 2008 (an additional 5% lower, compared to 1996), although the solar irradiance conditions were apparently similar. This provides an additional check on the magnitude of the geomagnetic component, showing that it can be significant, but that the effect is still a small fraction of the total change.

5. Discussion

[25] Solar EUV is the principal factor controlling the temperature and density of the thermosphere, but there could be other possible explanations for the observed anomalous densities during the recent solar minimum. Geomagnetic activity has been shown to cause part of these changes, but the magnetosphere provides too little energy to the thermosphere during solar minimum to be a major factor. Secular change due to radiative cooling by anthropogenic gases, primarily CO_2, also contributes, but is only significant on longer time scales than a single solar cycle. Propagation of changes in lower atmosphere circulation to the upper atmosphere can also be considered, but it is not likely that three anomalous years in a row could occur.

[26] The solar minimum between cycles 23/24 was anomalous with regard to its length as well as its depth. This may have specific ramifications for solar irradiance, but what of the terrestrial response? There is always the possibility that it takes longer for the thermosphere to equilibrate than previously thought, and that it was simply the length of the solar minimum period that caused the density declines. Thermospheric equilibration time has been investigated with model simulations, finding that the thermosphere fully equilibrates in about a month, regardless of initial conditions. There is no evidence in the measured time series indicating that the densities continued to decline during the extended solar minimum, rather, the model simulations adequately describe thermospheric density throughout 2008 as the quiet Sun persisted. The middle atmosphere, by comparison, takes longer to equilibrate than the thermosphere. If mesopause region atomic oxygen densities declined significantly, that could reduce thermospheric density by reducing the mean molecular mass and hence the effective thermospheric scale height. The comparisons of interminimum change as a function of altitude analyzed by *Emmert et al.* [2010] found that perturbing only the exospheric temperature parameter in a Bates-Walker temperature profile did not result in an adequate fit to the altitude profiles, but an improved fit could be obtained from adjusting lower-thermosphere composition by decreasing atomic oxygen. On this basis they proposed that composition change could be a contributing factor. If this were caused by mesopause region changes, it would not be captured by the TIE-GCM, with its 97 km lower boundary. However, the simulations shown in Figure 6d show good correspondence to the measured slope. In contrast to a Bates-Walker profile, EUV heating in the

TIE-GCM affects not only the exospheric temperature, but deposits energy throughout the thermosphere, especially below 200 km, where it changes the lower-thermosphere temperature profile. Whether or not the TIE-GCM does this in a physically realistic manner, it does achieve a good fit to the observed changes.

[27] The evidence that solar EUV during 2007–2009 was lower than previous solar minima is substantial. Estimates of the decrease vary from 4% (based on the $F_{10.7}$ index) to 10% (based on MgII c/w) to 15% (based on SEM measurements), so it is possible that the actual change lies somewhere in this range. Supporting evidence for the MgII c/w estimates is available from the H Lyman α composite time series [*Woods et al.*, 2000]. The spectral variations of interminimum EUV change are not well known, but the thermospheric global mean temperature and density at high altitude are not very sensitive to details of the solar spectrum, because they respond to the integrated EUV energy. The estimated 10% reduction in total EUV energy input employed here is an approximation to actual solar changes, but it produces a model result that is commensurate measured density change.

[28] If EUV did decrease by 10%, a reduction in ionospheric total electron content of ~15% would be expected, on the basis of these simulations. This should be detectable in long-term data sets such as from radar, ionosonde and GPS stations. It is not yet clear if such changes are reliably observed, but recent work [*Araujo-Pradere et al.*, 2011; *Liu et al.*, 2011] indicates that some changes did occur. Even though the ionospheric response to the recent solar minimum was the first evidence that something was different, this may have been due more to reduction of ionospheric altitude than density. Owing to the lower observed density, reduction in ionospheric altitudes must have occurred, regardless of the causative mechanisms. Our future work will compare model simulations with the available ionospheric measurements.

[29] Another imponderable regards the significance of the proxy indices employed for solar EUV estimation. We cannot evaluate whether the tendency of $F_{10.7}$ to reach a plateau at solar minimum, while other parameters continue to decrease or fluctuate, has some physical meaning for the Sun, or is just a feature of the relative contribution of active regions to the radio noise spectrum, or a quirk of the measurement analysis. It is noteworthy that the MgII c/w index employed here did not significantly depart from its historical range during 2007–2009, rather, it persisted at values that were only seen briefly during previous solar minima, thereby establishing lower 81 day and annual means. Perhaps solar EUV emissions were exhibiting similar behavior.

[30] Additional questions are why the Sun was different in the recent solar minimum, what the relationship to other forms of "low" solar activity may be, and to what extent other regions of the solar spectrum might be similarly affected. Low-latitude coronal holes were particularly prevalent during the declining phase of solar cycle 23 and the minimum of cycle 23/24, which could offer an explanation for the lower EUV irradiance [*Woods*, 2010]. However, the TIMED SEE solar 27 day rotational variations during solar minimum were not large, with 2–5% modulation in the 26–34 nm band and 5–20% in the 1–7 nm band. This result is consistent with analysis of low-latitude coronal hole areas from SOHO EUV images in 1996 and 2008; consequently, we estimate that the coronal holes may contribute up to 5% lower 26–34 nm irradiance in 2008 than in 1996. If the solar EUV irradiance was additionally lower, it could be due to a slow decline in quiet Sun radiance. This would imply reductions in MUV (200–300 nm) irradiance as well as the EUV and FUV, and also possibly at longer wavelengths. Solar cycle variation in the MUV is only a few percent, so direct measurement of interminimum differences will be difficult to detect at these wavelengths.

[31] Finally, it may be considered whether this EUV reduction has implications for the total solar irradiance (TSI). The EUV itself contributes an insignificant amount to TSI, only a few mW m^{-2}, as compared to 1360 W m^{-2}, or a few parts in a million. TSI varies by only about 1 W m^{-2} over the solar cycle, but longer-wave UV variation does contribute to TSI variation, so the possibility that solar UV irradiance in general was anomalously low during 2007–2009 cannot be ignored. If quiet Sun radiance changes were similar to solar cycle spectral variations, then a 10% decrease in EUV would correspond to a decrease in TSI of about 0.1 W m^{-2}. There is evidence that the TSI may have been 0.2 to 0.5 W m^{-2} lower in 2008 than 1996 [*Fröhlich*, 2009]; however, there are considerable uncertainties in this determination [e.g., *Lockwood*, 2010; *Gray et al.*, 2010], and one conflicting report of slightly higher TSI [*Mekaoui and Dewitte*, 2008]. Most of these TSI results have a stated uncertainty of about 100 ppm, or 0.14 W m^{-2}. Consequently, there is no consensus yet on how much the TSI is lower, or why it might be lower.

[32] During the long wait for the start of solar cycle 24, there was some speculation that the Sun was entering a new Maunder Minimum. Although this did not occur, the extended intercycle minimum period has given us an opportunity to investigate the solar and terrestrial aspects of low-activity periods. It is clear that the thermosphere-ionosphere system is evolving, but that we can no longer assume that its external forcing returns to the same level at each solar minimum. Owing to the importance of untangling solar effects from anthropogenic climate change at satellite orbital altitudes, an ongoing program of continuous, well-calibrated, solar ultraviolet irradiance measurements is therefore indicated.

[33] **Acknowledgments.** The authors thank John Emmert and colleagues for providing the thermospheric neutral density data. This research was supported by NASA grant NAG5-11408 to the University of Colorado, NASA grant NNX08AM74G to the University of Southern California, and NASA grants NNX10AF21G and NNX07AC61G to the National Center for Atmospheric Research. NCAR is supported by the National Science Foundation. SOHO is a project of international cooperation between ESA and NASA.

[34] Robert Lysak thanks the reviewers for their assistance in evaluating this paper.

References

Akmaev, R. A., and V. I. Fomichev (2000), A model estimate of cooling in the mesosphere and lower thermosphere due to the CO_2 increase over the last 3–4 decades, *Geophys. Res. Lett.*, *27*, 2113, doi:10.1029/1999GL011333.

Araujo-Pradere, E. A., R. Redmon, M. Fedrizzi, R. Viereck, and T. J. Fuller-Rowell (2011), Some characteristics of the ionospheric behavior during solar cycle 23/24 minimum, *Sol. Phys.*, doi:10.1007/s11207-011-9728-3.

Bailey, S. M., T. N. Woods, C. A. Barth, S. C. Solomon, L. R. Canfield, and R. Korde (2000), Measurements of the solar soft X-ray irradiance from the Student Nitric Oxide Explorer: First analysis and underflight calibrations, *J. Geophys. Res.*, *105*, 27,179, doi:10.1029/2000JA000188.

Barth, C. A., W. K. Tobiska, G. J. Rottman, and O. R. White (1990), Comparison of 10.7 cm radio flux with SME solar Lyman alpha flux, *Geophys. Res. Lett.*, *17*, 571, doi:10.1029/GL017i005p00571.

Bruinsma, S. L., and J. M. Forbes (2010), Anomalous behavior of the thermosphere during solar minimum observed by CHAMP and GRACE, *J. Geophys. Res.*, *115*, A11323, doi:10.1029/2010JA015605.

Chamberlin, P. C., T. N. Woods, D. A. Crotser, F. G. Eparvier, R. A. Hock, and D. L. Woodraska (2009), Solar cycle minimum measurements of the solar extreme ultraviolet spectral irradiance on 14 April 2008, *Geophys. Res. Lett.*, *36*, L05102, doi:10.1029/2008GL037145.

Chen, Y., L. Liu, and W. Wan (2011), Does the $F_{10.7}$ index correctly describe solar EUV flux during the deep solar minimum of 2007–2009?, *J. Geophys. Res.*, *116*, A04304, doi:10.1029/2010JA016301.

Coley, W. R., R. A. Heelis, M. R. Hairston, G. D. Earle, M. D. Perdue, R. A. Power, L. L. Harmon, B. J. Holt, and C. R. Lippincott (2010), Ion temperature and density relationships measured by CINDI from the C/NOFS spacecraft during solar minimum, *J. Geophys. Res.*, *115*, A02313, doi:10.1029/2009JA014665.

Didkovsky, L. V., D. L. Judge, and S. R. Wieman (2010), Minima of solar cycles 22/23 and 23/24 as seen in SOHO/CELIAS/SEM absolute solar EUV flux, in *SOHO-23: Understanding a Peculiar Solar Minimum*, *ASP Conf. Series*, vol. 428, edited by S. R. Cranmer, J. T. Hoeksema, and J. Kohl, p. 73, Astron. Soc. of the Pac., San Francisco, Calif. (Available at http://arxiv.org/PS_cache/arxiv/pdf/0911/0911.0870v1.pdf.)

Eddy, J. A. (1976), The Maunder Minimum, *Science*, *192*, 1189, doi:10.1126/science.192.4245.1189.

Emmert, J. T. (2009), A long-term data set of globally averaged thermospheric total mass density, *J. Geophys. Res.*, *114*, A06315, doi:10.1029/2009JA014102.

Emmert, J. T., J. M. Picone, J. L. Lean, and S. H. Knowles (2004), Global change in the thermosphere: Compelling evidence of a secular decrease in density, *J. Geophys. Res.*, *109*, A02301, doi:10.1029/2003JA010176.

Emmert, J. T., J. M. Picone, and R. R. Meier (2008), Thermospheric global average density trends, 1967–2007, derived from orbits of 5000 near-Earth objects, *Geophys. Res. Lett.*, *35*, L05101, doi:10.1029/2007GL032809.

Emmert, J. T., J. L. Lean, and J. M. Picone (2010), Record-low thermospheric density during the 2008 solar minimum, *Geophys. Res. Lett.*, *37*, L12102, doi:10.1029/2010GL043671.

Fröhlich, C. (2009), Evidence of a long-term trend in total solar irradiance, *Astron. Astrophys.*, *501*, L27, doi:10.1051/0004-6361/200912318.

Gibson, S. E., J. U. Kozyra, G. de Toma, B. A. Emery, T. Onsager, and B. J. Thompson (2009), If the Sun is so quiet, why is the Earth ringing? A comparison of two solar minimum intervals, *J. Geophys. Res.*, *114*, A09105, doi:10.1029/2009JA014342.

Gray, L. J., et al. (2010), Solar influences on climate, *Rev. Geophys.*, *48*, RG4001, doi:10.1029/2009RG000282.

Hagan, M. E., R. G. Roble, and J. Hackney (2001), Migrating thermospheric tides, *J. Geophys. Res.*, *106*, 12,739, doi:10.1029/2000JA000344.

Heelis, R. A., W. R. Coley, A. G. Burrell, M. R. Hairston, G. D. Earle, M. D. Perdue, R. A. Power, L. L. Harmon, B. J. Holt, and C. R. Lippincott (2009), Behavior of the O^+/H^+ transition height during the extreme solar minimum of 2008, *Geophys. Res. Lett.*, *36*, L00C03, doi:10.1029/2009GL038652.

Judge, D. L., et al. (1998), First solar EUV irradiances obtained from SOHO by the CELIAS/SEM, *Sol. Phys.*, *177*, 161, doi:10.1023/A:1004929011427.

Keating, G. M., R. H. Tolson, and M. S. Bradford (2000), Evidence of long-term global decline in the Earth's thermospheric densities apparently related to anthropogenic effects, *Geophys. Res. Lett.*, *27*, 1523, doi:10.1029/2000GL003771.

Keeling, C. D., and T. P. Whorf (2005), Atmospheric CO_2 Records From Sites in the SIO Air Sampling Network, http://cdiac.ornl.gov/trends/co2/sio-keel.html, Carbon Dioxide Inf. Anal. Cent., Oak Ridge Natl. Lab. DAAC, Oak Ridge, Tenn.

Laštovička, J., R. A. Akmaev, G. Beig, J. Bremer, and J. T. Emmert (2006), Global change in the upper atmosphere, *Science*, *314*, 1253, doi:10.1126/science.1135134.

Laštovička, J., R. A. Akmaev, G. Beig, J. Bremer, J. T. Emmert, C. Jacobi, M. J. Jarvis, G. Nedoluha, Y. I. Portnyagin, and T. Ulich (2008), Emerging pattern of global change in the upper atmosphere and ionosphere, *Ann. Geophys.*, *26*, 1255, doi:10.5194/angeo-26-1255-2008.

Lei, J., J. P. Thayer, J. M. Forbes, E. K. Sutton, and R. S. Nerem (2008), Rotating solar coronal holes and periodic modulation of the upper atmosphere, *Geophys. Res. Lett.*, *35*, L10109, doi:10.1029/2008GL033875.

Liu, L., Y. Chen, H. Le, V. I. Kurkin, N. M. Polekh, and C.-C. Lee (2011), The ionosphere under extremely prolonged low solar activity, *J. Geophys. Res.*, *116*, A04320, doi:10.1029/2010JA016296.

Lockwood, M. (2010), Solar change and climate: An update in the light of the current exceptional solar minimum, *Proc. R. Soc., Ser. A*, *466*, 303, doi:10.1098/rspa.2009.0519.

Lühr, H., and C. Xiong (2010), IRI-2007 model overestimates electron density during the 23/24 solar minimum, *Geophys. Res. Lett.*, *37*, L23101, doi:10.1029/2010GL045430.

Marcos, F. A., J. O. Wise, M. J. Kendra, N. J. Grossbard, and B. R. Bowman (2005), Detection of a long-term decrease in thermospheric neutral density, *Geophys. Res. Lett.*, *32*, L04103, doi:10.1029/2004GL021269.

Mekaoui, S., and S. Dewitte (2008), Total solar irradiance measurement and modelling during solar cycle 23, *Sol. Phys.*, *247*, 203, doi:10.1007/s11207-007-9070-y.

Picone, J. M., A. E. Hedin, D. P. Drob, and A. C. Aikin (2002), NRLMSISE-00 empirical model of the atmosphere: Statistical comparisons and scientific issues, *J. Geophys. Res.*, *107*(A12), 1468, doi:10.1029/2002JA009430.

Qian, L., R. G. Roble, S. C. Solomon, and T. J. Kane (2006), Calculated and observed climate change in the thermosphere, and a prediction for solar cycle 24, *Geophys. Res. Lett.*, *33*, L23705, doi:10.1029/2006GL027185.

Qian, L., S. C. Solomon, and T. J. Kane (2009), Seasonal variation of thermospheric density and composition, *J. Geophys. Res.*, *114*, A01312, doi:10.1029/2008JA013643.

Qian, L., J. Laštovička, R. G. Roble, and S. C. Solomon (2011), Progress in observations and simulations of global change in the upper atmosphere, *J. Geophys. Res.*, *116*, A00H03, doi:10.1029/2010JA016317.

Richards, P. G., J. A. Fennelly, and D. G. Torr (1994), EUVAC: A solar EUV flux model for aeronomic calculations, *J. Geophys. Res.*, *99*, 8981, doi:10.1029/94JA00518.

Richmond, A. D., E. C. Ridley, and R. G. Roble (1992), A thermosphere/ionosphere general circulation model with coupled electrodynamics, *Geophys. Res. Lett.*, *19*, 601, doi:10.1029/92GL00401.

Rishbeth, H., and R. G. Roble (1992), Cooling of the upper atmosphere by enhanced greenhouse gases: Modeling of thermospheric and ionospheric effects, *Planet. Space Sci.*, *40*, 1011, doi:10.1016/0032-0633(92)90141-A.

Roble, R. G., and R. E. Dickinson (1989), How will changes in carbon dioxide and methane modify the mean structure of the mesosphere and thermosphere?, *Geophys. Res. Lett.*, *16*, 1441, doi:10.1029/GL016i012p01441.

Roble, R. G., E. C. Ridley, A. D. Richmond, and R. E. Dickinson (1988), A coupled thermosphere/ionosphere general circulation model, *Geophys. Res. Lett.*, *15*, 1325, doi:10.1029/GL015i012p01325.

Russell, C. T., J. G. Luhmann, and L. K. Jian (2010), How unprecedented a solar minimum?, *Rev. Geophys.*, *48*, RG2004, doi:10.1029/2009RG000316.

Solomon, S. C., and L. Qian (2005), Solar extreme-ultraviolet irradiance for general circulation models, *J. Geophys. Res.*, *110*, A10306, doi:10.1029/2005JA011160.

Solomon, S. C., S. M. Bailey, and T. N. Woods (2001), Effect of solar soft X-rays on the lower ionosphere, *Geophys. Res. Lett.*, *28*, 2149, doi:10.1029/2001GL012866.

Solomon, S. C., T. N. Woods, L. V. Didkovsky, J. T. Emmert, and L. Qian (2010), Anomalously low solar extreme-ultraviolet irradiance and thermospheric density during solar minimum, *Geophys. Res. Lett.*, *37*, L16103, doi:10.1029/2010GL044468.

Viereck, R. A., L. E. Floyd, P. C. Crane, T. N. Woods, B. G. Knapp, G. Rottman, M. Weber, L. C. Puga, and M. T. DeLand (2004), A composite Mg II index spanning from 1978 to 2003, *Space Weather*, *2*, S10005, doi:10.1029/2004SW000084.

Viereck, R. A., M. Snow, M. T. DeLand, M. Weber, L. Puga, and D. Bouwer (2010), Trends in solar UV and EUV irradiance: An update to the MgII Index and a comparison of proxies and data to evaluate trends of the last 11 year solar cycle, Abstract GC21B-0877 presented at 2010 Fall Meeting, AGU, San Francisco, Calif., 13–17 Dec.

Woods, T. N. (2010), Irradiance variations during this solar cycle minimum, in *SOHO-23: Understanding a Peculiar Solar Minimum*, *ASP Conf. Series*, vol. 428, edited by S. R. Cranmer, J. T. Hoeksema, and J. Kohl, p. 68, Astron. Soc. of the Pac., San Francisco, Calif.

Woods, T. N., and G. J. Rottman (2002), Solar ultraviolet variability overtime periods of aeronomic interest, in *Atmospheres in the Solar System: Comparative Aeronomy*, *Geophys. Monogr. Ser.*, vol. 130, edited by M. Mendillo, A. Nagy, and J. H. Waite Jr., p. 221, AGU, Washington, D. C.

Woods, T. N., and G. Rottman (2005), The XUV photometer system (XPS): Solar variations during the SORCE mission, *Sol. Phys.*, *230*, 345, doi:10.1007/s11207-005-4119-2.

Woods, T. N., G. J. Rottman, S. M. Bailey, S. C. Solomon, and J. Worden (1998), Solar extreme ultraviolet irradiance measurements during solar cycle 22, *Sol. Phys.*, *177*, 133, doi:10.1023/A:1004912310883.

Woods, T. N., W. K. Tobiska, G. J. Rottman, and J. R. Worden (2000), Improved solar Lyman α irradiance modeling from 1947 through 1999 based on UARS observations, *J. Geophys. Res.*, *105*, 27,195, doi:10.1029/2000JA000051.

Woods, T. N., F. G. Eparvier, S. M. Bailey, P. C. Chamberlin, J. Lean, G. J. Rottman, S. C. Solomon, W. K. Tobiska, and D. L. Woodraska (2005), Solar EUV Experiment (SEE): Mission overview and first results, *J. Geophys. Res.*, *110*, A01312, doi:10.1029/2004JA010765.

Woods, T. N., P. C. Chamberlin, J. Harder, R. A. Hock, M. Snow, F. G. Eparvier, J. Fontenla, W. E. McClintock, and E. C. Richard (2009), Solar Irradiance Reference Spectra (SIRS) for the 2008 Whole Heliosphere Interval (WHI), *Geophys. Res. Lett.*, *36*, L01101, doi:10.1029/2008GL036373.

L. V. Didkovsky, Space Sciences Center, University of Southern California, Stauffer Hall of Science, 835 Bloom Walk, Los Angeles, CA 90089, USA.

L. Qian and S. C. Solomon, High Altitude Observatory, National Center for Atmospheric Research, 1850 Table Mesa Dr., Boulder, CO 80307, USA. (stans@ucar.edu)

R. A. Viereck, Space Weather Prediction Center, NOAA, 325 Broadway, Boulder, CO 80305, USA.

T. N. Woods, Laboratory for Atmospheric and Space Physics, University of Colorado at Boulder, 1234 Innovation Dr., Boulder, CO 80309, USA.